Current Applied Physics 16 (2016) 691–695

Contents lists available at ScienceDirect

Current Applied Physics

journal homepage: www.elsevier.com/locate/cap

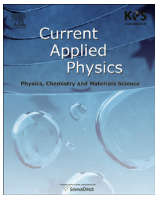

Comparison of hydrogen sulfide gas and sulfur powder for synthesis of molybdenum disulfide nanosheets

Jusang Park [a], Jeong-Gyu Song [a], Taejin Choi [a], Sangwan Sim [a], Hyunyong Choi [a], Sang Wook Han [b], Han-Bo-Ram Lee [c], Soo-Hyun Kim [d], Hyungjun Kim [a, *]

[a] *School of Electrical and Electronic Engineering, Yonsei University, Seoul 120-749, South Korea*
[b] *Department of Physics and Energy Harvest–Storage Research Center, University of Ulsan, Ulsan 680-749, South Korea*
[c] *Materials Science and Engineering, Incheon National University, Incheon 406-840, South Korea*
[d] *School of Materials Science and Engineering, Yeungnam University, Gyeongsan-si 712-749, South Korea*

ARTICLE INFO

Article history:
Received 29 July 2015
Received in revised form
12 February 2016
Accepted 31 March 2016
Available online 1 April 2016

Keywords:
Hydrogen sulfide
Sulfur powder
Transition metal dichalcogenides (TMDC)
2D nanosheet
Selectable area growth

ABSTRACT

Layered transition metal dichalcogenides (TMDCs) have the potential to be used as an alternative to graphene in nano applications, because of their unique opto-electric properties. However, the large-scale synthesis of TMDCs has not been thoroughly investigated with different sulfurization agents, nor have the effects of defects and vacancies on such synthesis been determined. This study therefore looks at the synthesis of MoS_2 nanosheets from a thin Mo film to compare the effects of using H_2S gas or sulfur powder as the sulfurization agent. In either case, a four-layered nanosheet is obtained; however, the good stoichiometry of MoS_2, smallest defects, and fewest vacancies are obtained using H_2S.

1. Introduction

Layered transition metal dichalcogenides (TMDCs) have recently drawn significant attention for use as next generation nanoelectronics [1], thin film transistors [2], logic circuits [3], sensors [4], catalysts [5,6], and optoelectronic devices [7,8]. The physical, electrical, and optical properties of TMDCs have so far mostly been studied through physical exfoliation of nanosheets and their transfer onto suitable substrates [9–11]. However, nanosheets with a large surface area can only be achieved through synthesis directly onto a substrate. Recently, the layered MoS_2 was most famous in TMDCs because the exotic properties of optical and electrical. The early stage method of synthesizing MoS_2 is the sulfurization of metal and metal-oxide films using a sulfurization agent [12–16], and good quality MoS_2 and WS_2 nanosheets have been achieved through chemical vapor deposition (CVD) [17–20].

There is a potential problem in the use of sulfur powder as a sulfurization agent, namely the fact that its vaporization requires temperatures above 200 °C, and that its vapor has a S_8 crown ring structure that leads to inhomogeneous sulfurization [21]. In contrast, H_2S gas has a simple molecular structure with a low decomposition energy, ensuring a reliable and homogeneous reaction [22,23]. The synthesis of MoS_2 nanostructures has been previously achieved using H_2S gas [24, 25], but was found to result in S vacancies forming near nanocluster edges, grain boundaries, and defect sites [26, 27, 28] that greatly affected the optical and electrical properties [27, 28]. However, as there has been no comparative study of different sulfurization agents, this study compares the synthesis of MoS_2 using H_2S gas with that using sulfur powder at temperatures of 1000 and 750 °C. The intrinsic properties of the MoS_2 nanosheets obtained are also investigated through pump probe measurements, though the ease with which MoS_2 readily changes its electrical properties prevented these from being included.

2. Experimental section

The single-crystal SiO_2 and MgO substrates were prepared by ultrasonic cleaning in acetone, IPA, and DI water for 10 min each. For metal sulfurization, 5 or 10 nm Mo metal films were deposited by sputtering for 5 or 10 s, respectively. Fig. 1 (a) shows the

---

* Corresponding author.
E-mail address: hyungjun@yonsei.ac.kr (H. Kim).

http://dx.doi.org/10.1016/j.cap.2016.03.022
1567-1739/

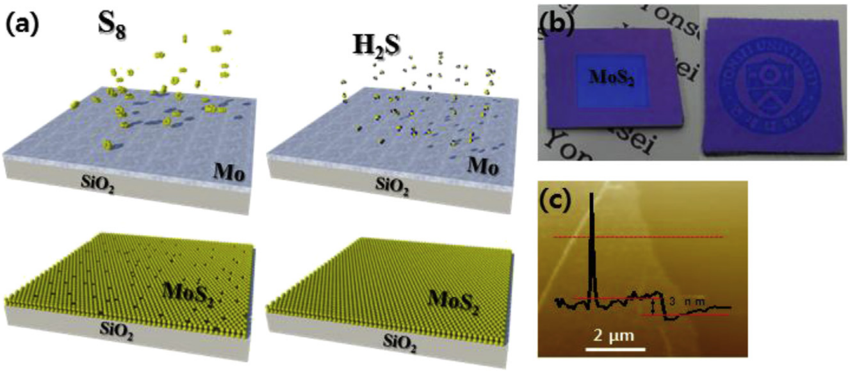

Fig. 1. (a) Schematic illustration of the sulfurization process. (b) Optical images of MoS_2 layers grown on a SiO_2 substrate. (c) AFM image of a four-layer MoS_2 nanosheet ~4 nm in thickness on a SiO_2/Si substrate.

differences in the sulfurization process depending on whether initial sulfurization in a tube type furnace at 500 °C was carried out using 5 sccm of H_2S gas or 3 g of sulfur powder (introduced at 120 °C) under a 50 sccm flow of Ar. Following this initial sulfurization, the temperature was increased to 750 or 1000 °C and held for 10 min to enhance the quality of the MoS_2 nanosheet. The sample preparation conditions are summarized in Fig. 2.

To measure the thickness of the MoS_2 nanosheets produced, each was measured by atomic force microscopy (AFM). Differences between the two different sulfurization methods were assessed by characterizing the different nanosheets using Raman spectroscopy, X-ray photoemission spectroscopy (XPS), tunneling electron microscopy (TEM), and pump probe measurement. The XPS measurements were performed at the 09A beam line of the National Synchrotron Radiation Research Center (NSRRC) in Hsinchu, Taiwan, with all data being obtained at a base pressure of less than 1×10^{-9} mbar.

The electrical characteristics and physical properties of the MoS_2 nanosheet were analyzed using ultrafast pump-probe methods so as to prevent any contamination or damage. These measurements were carried out with a visible probe range based on a 250 KHz Ti:sapphire laser system (Coherent RegA 9050) producing 50 fs pulses at 800 nm. A white-light continuum was created by focusing these 800 nm pulses into a sapphire disk, with 400 nm pulses being generated by a second harmonic.

3. Results and discussion

As shown in Fig. 1(b), large-area MoS_2 nanosheet with a uniform color was selectively grown using H_2S gas. After transferring it onto a clean SiO_2 substrate, an AFM line profile (Fig. 1(c)) was used to determine its thickness as 3 nm, which equates to four layers of MoS_2 nanosheet.

Fig. 2(a) shows the Raman spectra of MoS_2 nanosheets, prepared under various conditions (Fig. 2), from which the width of each peak can be used to determine the crystallinity of the sample [29, 30]. That is, the 24 cm^{-1} gap between the $E^1{}_{2g}$ and $A^1{}_g$ peaks corresponds to four layers of the MoS_2 nanosheet [30], and therefore confirms the AFM-measured thickness. Note also that the Si peak is normalized to allow such comparison between the intensities and widths of the $E^1{}_{2g}$ and A_{1g} peaks. Fig. 2(b) shows the peak distance as a function of the Mo film thickness, suggesting a strong relation between the thickness of the MoS_2 nanosheets and the Mo films. There is, however, a poor conformity to the Raman spectrum when the number of layers exceeds four, with the larger intensity ratio of sample H10 indicating that a good crystallinity can be obtained by annealing at 1000 °C with H_2S gas. The full-width at half maximum (FWHM) values of the Raman peak given in Fig. 2(c) reveal that the width of the $E^1{}_{2g}$ peak relative to that of the A_{1g} peak is lower in the synthesized MoS_2 nanosheet than in mechanically exfoliated-MoS_2 (the black dotted line), which can be attributed to planar vibration ($E^1{}_{2g}$) being strongly related to the randomly distributed grains found in CVD-grown MoS_2 nanosheets [13]. The FWHM values and peak intensities are also much higher at 750 °C than at 1000 °C, especially when H_2S gas is used for sulfurization.

The quality and crystallinity of the MoS_2 nanosheet were assessed by TEM, with Fig. 3(a,b) showing the nanosheet prior to sulfurization. The use of H_2S (Fig. 3(d,f)) was found to produce an enhanced crystallinity when compared to using sulfur powder at the same annealing temperature (Fig. 3(c,e)). The diffraction patterns and FWHM in the insets of Fig. 3(c–f) show evidence of a six-fold-symmetry following sulfurization [13, 31], with the ring pattern of sample H10 indicating a polycrystalline structure.

The XPS results for the Mo 3*d* and S 2*p* core-levels of samples S7, H7, S10, and H10 are shown in Fig. 4, from which the atomic ratio (stoichiometry) of each sample was obtained based on the ratio of the Mo 3*d* peaks intensity to that of the S 2*p* peak. As shown in Fig. 2, samples prepared in H_2S gas had a comparable atomic concentration to bulk MoS_2, whereas the use of sulfur powder resulted in concentrations either under (750 °C) or over (1000 °C) stoichiometry. This non-stoichiometry is believed to be caused by vacancies and defects generated during synthesis [26, 27, 28]. With either sulfurization agent, the width of the Mo 3*d* and S 2*p* core-level peaks roughly doubled; however, with only sulfur powder, the Mo 3*d* core levels exhibited a peak suggesting oxidization to MoO_3 at a higher binding energy. This phenomenon most likely originates from the substrate, with the oxygen species produced believed to interrupt the crystal structure and degrade the electrical properties of the thin film. This suggests that the use of H_2S gas is the more suitable option for the synthesis of MoS_2 nanosheets.

To further confirm the superiority of H_2S gas over sulfur powder, ultrafast optical-pump-probe measurements of the carrier relaxation time were performed. For this, four different samples of MoS_2 nanosheet were prepared on MgO substrates under conditions of: H_2S at 750 °C (Sample **I**), sulfur powder at 750 °C (Sample **II**), H_2S gas at 1000 °C (Sample **III**), and sulfur powder at 1000 °C (Sample **IV**). A MgO (100) substrate was used as this is not excited by probing measurements with a large band gap of 7.8 eV, as transparent substrates need a band gap larger than the photon energy (3.01 eV) of the pump pulses used for measurement.

Prior to pump-probe measurement, the ground state absorption was measured to determine an appropriate pump-probe wavelength. As can be seen in Fig. 5 (a), the A and B excitons are